MA Load Current Multiplier*

V. A. Kokshenev[1], A. A. Kim[1,2], B. M. Kovalchuk[1],
A. V. Fedunin[1], F. I. Fursov[1], N. E. Kurmaev[1], A. Yu. Labetsky[1], A. V. Shishlov[1,2]
A. S. Chuvatin[3]

[1]*Institute of High Current Electronics, Academichesky Ave. 2/3, Tomsk, 634055, Russia*
Phone: (3822) 492-908, Fax: (3822) 492-751, E-mail: vak@oit.hcei.tsc.ru
[2]*Tomsk Polytechic University, Lenina Ave. 30, 634050 Tomsk, Russia*
[3]*Laboratoire de Physique et Technologie des Plasmas, Ecole Polytechnique, Palaiseau, 91128, France*

Abstract – The concept of the Load Current Multiplier (LCM) is proposed to improve the generator-to-load coupling and to increase the energy transfer efficiency into pulse-power loads [1]. The LCM is being tested on GIT12 generator and the work is divided into two steps. The first step was to manufacture and test the coreless LCM with the objective to verify the LCM concept, to check if the LCM is capable to drive a z-pinch load, and to investigate possible drawbacks. It was found that in the tests with static inductive load the observed load current was ~1.8 times the generator current. In the case of triple Ne gas puff, a typical dynamic of the z-pinch implosion was observed. These results are promising for the next step of the work, which is the design and testing of the LCM with a ferromagnetic core.

1. Design of the coreless LCM

The coreless LCM designed for the GIT12 is a current transformer with a primary winding including 2 turns and a secondary winding of 1 turn. The output part of the GIT12 with LCM upstream from the load is shown in Fig. 1. The inductance of the lines, ρ_1 and ρ_2 , that are connected in series to the GIT12 Marxes and in parallel to the load, is the primary leakage inductance, ΔL. It is added to the Marx inductance and therefore has to be as small as possible. On the other hand, the interelectrode gaps in these lines are limited by insulation considerations, but mainly by assembly tolerance. In Fig. 1, these gaps are typically 1.5 – 2.5 cm resulting in ΔL ~ 21 nH.

The primary inductance of the LCM is determined by the geometry of the torus between the lines ρ_1 and ρ_2. It is connected in parallel to the load, and therefore the current flowing in this inductance represents the loss current. Below this inductance is referred as a loss inductance, L_{LOSS}. In the coreless LCM in Fig. 1, it equals to L_{LOSS} = 143 nH.

The post-hole convolute at the output of the LCM consists of twelve 25 mm diameter posts locating in the center of 50 mm diameter holes.

The diagnostics includes the B-dots, measuring the LCM input current *Iin*, the diode current *Id*, and the LCM output current *Iout*. The total Marx current, *IG*, is measured as a sum of currents at the output of each of 12 Marxes.

The diameter of the LCM is ~160 cm, the height is 60 cm. The total weight of the LCM hardware is ~1000 kg.

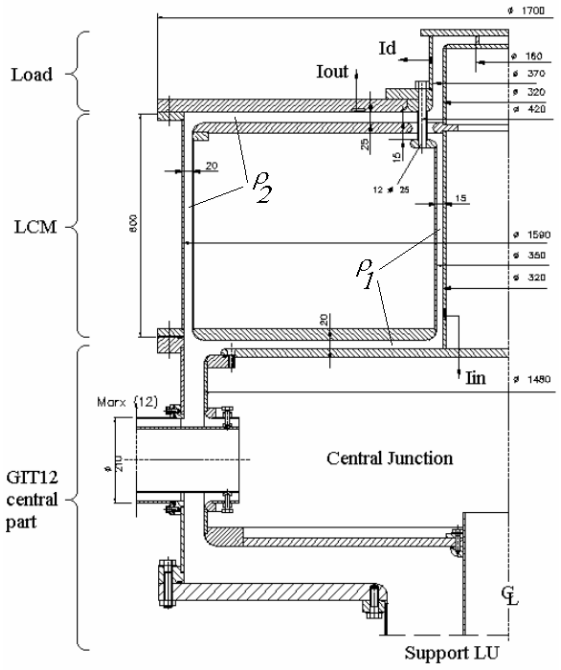

Fig. 1. The coreless LCM on the GIT12 generator

Figure 2 shows simulated LCM performance at 50 kV Marx charge voltage allowing to compare the expected diode current with the current *Id_INI*, which is the standard GIT12 diode current without the LCM. In LCM configuration, the rise time increases from ~1.8 us to ~ 2.1 us due to additional ΔL and fourfold inductance of the load, which sees the generator. The predicted LCM gain, $K = Id/Iin$, is 1.87. At t = 1 us, the current *Id_INI* ~3.7 MA, whereas the current Id = 4.9 MA. In case of the gas puff load with implosion time

* The work is supported by DGA/Centre d'Etudes de Gramat, France, through a contract with AASC, USA.

of t_{IMP} ~ 1 us, it means that the advantage of using the coreless LCM is *Id/Id_INI* ~ 1.3 or less, depending on exact t_{IMP}.

Nevertheless, to reduce the risk in verifying the LCM concept, checking its capability to drive the z-pinch load, and investigating possible drawbacks, the conservative design presented in Fig. 1 was produced and tested in experiments described below.

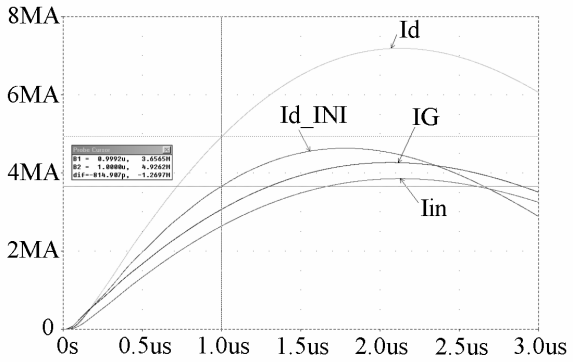

Fig. 2. Simulated currents in LCM configuration compared with standard GIT12 diode current, *Id_INI*

2. Test with static inductive load

In this test the inductance of the static load downstream from the LCM post-hole convolute was 8 nH. Test was performed at 30 kV and 50 kV Marx charge voltage. The results are shown in Fig. 3, where the recorded currents and the gain, *K*, are presented. At *t* = 1 us the diode current at 50 kV charge, *Id_50*, reaches ~ 4.5 MA, at *t* ~ (1.4 – 1.6) us the recorded traces stop to rise indicating a breakdown in the system. Nevertheless, the LCM gain, *K* ~ 1.8, is approximately constant during more than 2 us. This shows that the breakdown occurs not in the LCM hardware, but somewhere upstream.

The reason for this breakdown is the increased voltage at the output of the Marxes due to larger downstream inductance in configuration with LCM compared to standard GIT12 design. This conclusion was confirmed after the system was disassembled and several flashover spots were observed on the vacuum surface of the oil-vacuum Marx interfaces.

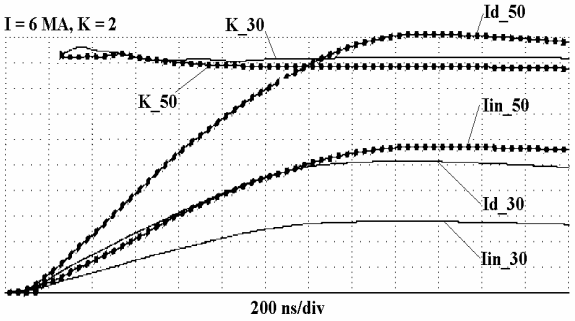

Fig. 3. Test with 8 nH inductive load at 30 kV and 50 kV Marx charge voltage

3. Test with a triple Ne gas puff

3.1. Gas puff hardware and diagnostics

The experiments were carried out with the Ne triple gas puff, whose two outer shells are annular gas puffs, and the inner cascade is a solid fill gas jet along the system axis. The diameters of the shells are 240 mm/100 mm/20 mm (in two shots, the triple gas puffs with shell diameters of 270 mm/100 mm/20 mm and 160 mm/80 mm/20 mm were used). They are formed by pulsed gas injection through the supersonic nozzles into the interelectrode gap by using the electromagnetic valve. The gas was injected from the anode (nozzles) towards the cathode, which is the stainless-steel wire mesh with 81% transparency. The mass of the shells was set by adjusting the gas valve plenum pressure and the time delay between the gas valve opening and triggering the generator.

The length of the gas puff was 2 cm. The design of the load unit is shown in Fig. 3.

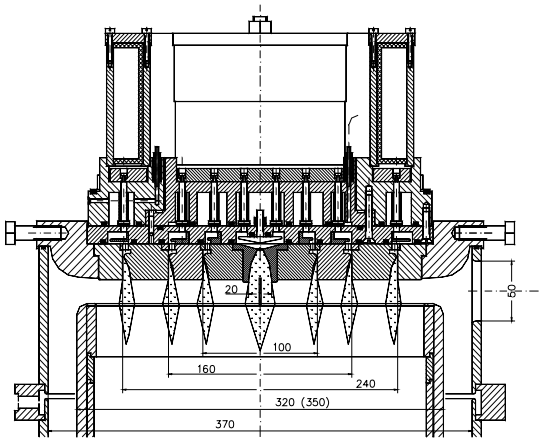

Fig. 3. Design of the load unit allowing simultaneous creation up to 4 cascades of a gas puff

Implosion dynamics was recorded by a visible light streak camera with a writing speed of 125 ns/cm. The inlet slit of the streak camera was aligned normal to the z-pinch axis in the middle of the anode-cathode gap. The streak camera views a region near the z-pinch axis with the diameter of 5 cm.

The pinch image in the final stage of implosion was registered by two time-integrated pinhole cameras. The first pinhole camera was filtered by Beryllium 25 μm + Polypropylene 10 μm and had rather high sensitivity in the region of neon K-lines. The second pinhole camera was set to register the neon recombination radiation and had the filter of Teflon 15 μm + Aluminum 0.2 μm + Kinfoil 2 μm.

The instant of gas puff implosion was registered by appearance of the x-ray radiation pulse from the neon plasma. For the x-ray radiation measurements, an x-ray vacuum diode (XRD) with an aluminum

photocathode placed behind a filter of Kinfoil 6 μm + Al 0.6 μm was used.

3.2.Performance of the GIT12 with coreless LCM driving the Z-pinch load

The capability of the GIT12 with LCM to drive a Z-pinch load means the absence of breakdowns in the LCM hardware and the absence of extra current losses in L_{LOSS} during a short-time voltage increase (up to ~700-800 kV) when the pinch implodes on the axis.

Figure 4 shows the currents, the LCM gain, the XRD signal, and the energy, *E*, transferred to the load (calculated from recorded currents in assumption that the load does not have resistive component) in shot #797 at 49 kV Marx charge voltage. This shot was made with the triple Ne gas puff (240/100/20 mm diam, 200/150/150 μg/cm mass, preliminary estimation). The peak diode current is ~4 MA, the implosion time is 960 ns.

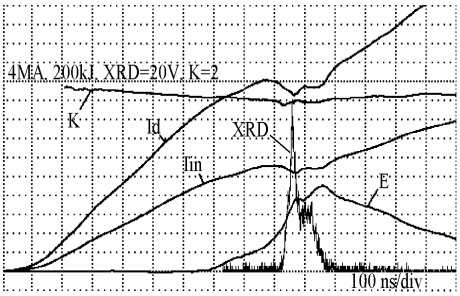

Fig. 4. Currents, energy transferred into the load, XRD signal, and the LCM gain in shot #797

This shot was simulated in Pspice (Fig. 5) by using a 0D slug model with infinite thin shells. In simulation, the gas puff implodes to the final diameter of 6 mm, which is kept constant from this point on. The central gas jet is not taken into account (it does not influence the results of simulations in this approximation). To get the same implosion time as that in the test, the simulation requires the mass of (150/150) ug/cm for the two outer shells.

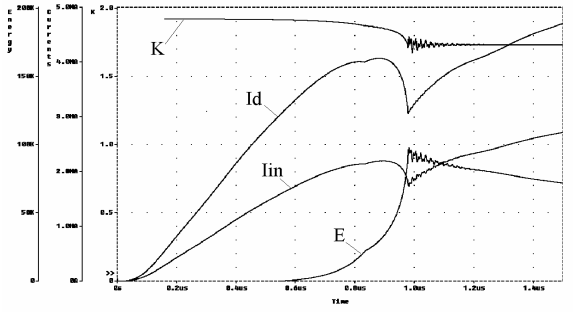

Fig. 5. Shot #797 simulated in Pspice

The overall behavior of the traces in Figs. 4 and 5 is similar. The diode currents, *Id*, reach the same peak value of ~ 4 MA, the transferred energy is ~80 kJ in experiment and ~96 kJ in simulation. The LCM gain, *K*, is ~1.9 at the beginning and reduces to ~1.75 to the time of implosion due to an increase in the load inductance resulting in more current flowing in L_{LOSS}. All these indicate that there are no breakdowns in the LCM hardware.

The main difference is that the current drop at implosion in simulation is much deeper than that in experiment. This indicates that at implosion the whole diode current does not flow inside the area with diameter of 6 mm, as this is assumed in simulation. It seems to be a special feature of a large diameter gas puff implosion rather than some failure in the LCM operation.

Other difference, which is not clear at the moment, is the lower mass of the shells in simulations compared to the experiment. In other words, the implosion occurs faster and at lower current than predicted. This peculiarity was observed not only in simple model described above but also in other models, like 0D show plow which takes into account the initial gas distribution between the three shells or direct solution of the circuit equations.

3.3. Z-pinch implosion dynamics

Despite the fact that the gas puff implosion occurred at a lower current amplitude than expected, a typical implosion dynamics of the multi-shell gas puff is observed in the streak camera. The pinhole cameras register an image of the pinch formed on the axis. Figure 6 shows these pictures in shot #797 with the coreless LCM. It can be compared with Fig. 7, where the same pictures obtained in shot #766 in similar conditions (see Table 1) without the LCM are presented.

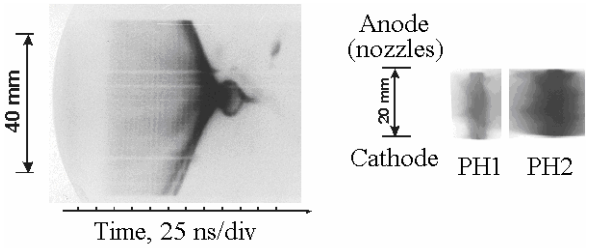

Fig. 6. Streak camera picture and pinhole camera images obtained in shot #797 with the coreless LCM

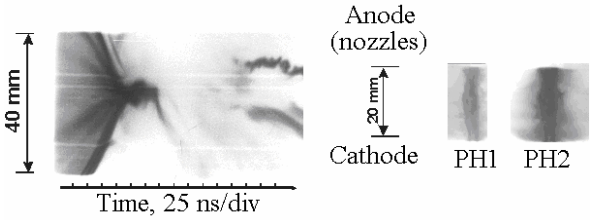

Fig. 7. Streak camera picture and pinhole camera images obtained in shot #766 without the LCM

Table I. Summary of the shots performed with the triple Ne gas puff

Shot#	D_{OUT} mm	D_{MIDT} mm	D_{IN} mm	M_{OUT} ug/cm	M_{MID} ug/cm	M_{IN} ug/cm	I_d max MA	t_{IMP} ns	Config
792	240	100	20	135	150	150	3.2	958	LCM
793	240	100	20	200	150	150	3.9	1000	LCM
794	240	100	20	300	150	150	3.9	10004	LCM
795	240	100	20	200	150	150	3.8	998	LCM
796	240	100	20	300	300	150	3.2	>1600	LCM
797	240	100	20	200	150	150	4.0	869	LCM
798	240	100	20	300	150	150	4.3	907	LCM
799	240	100	20	400	200	200	4.5	1016	LCM
800	270	100	20	290	200	125	5.1	1000	LCM
801	160	80	20	400	250	100	3.9	885	LCM
766	240	100	20	155	135	145	3.7	1030	No LCM
759	270	80	20	200	205	145	4.0	1151	No LCM
637	160	80	20	250	250	100	3.5	998	No LCM

In the table, the implosion time t_{IMP} is determined as a time between the current I_d reaches 100 kA and the time the XRD radiation pulse peaks.

There were 10 shots with gas puff performed in total on GIT12 with the coreless LCM. The results are summarized in Table 1. The last three shots in this table are shown for comparison, they were made without the LCM.

4. Conclusion

The LCM is proven to be able to increase the MA level load current as compared to the generator current, and to drive successfully the dynamic z-pinch load. The observed LCM gain is close to the predicted one, the current losses in the LCM post-hole convolute are negligible.

In the experiments described above, the real advantage of using the LCM is rather small because the conservative design of the coreless LCM in Fig. 1 introduces too large inductance into the GIT12 discharge circuit. It is evident that the design has to be optimized by reducing the primary leakage inductance and by increasing the inductance L_{LOSS}. Both these goals can be reached by using the LCM with a ferromagnetic core.

Reference

[1] A.S. Chuvatin, et al., *in Proc. 15th Inter. Conf. High-power particle beams*, 2004, p. 381.